Journal of Alloys and Compounds 497 (2010) 373–376

Contents lists available at ScienceDirect

Journal of Alloys and Compounds

journal homepage: www.elsevier.com/locate/jallcom

Preparation, characterization and photocatalytic activity of Co-doped ZnO powders

Chao Xu, Lixin Cao*, Ge Su, Wei Liu, Xiaofei Qu, Yaqin Yu

Institute of Materials Science and Engineering, Ocean University of China, Songling Road 238, Qingdao 266100, Shandong Province, PR China

ARTICLE INFO

Article history:
Received 25 October 2009
Received in revised form 3 March 2010
Accepted 4 March 2010
Available online 15 March 2010

Keywords:
ZnO
Hydrothermal
Characterization
Photocatalytic

ABSTRACT

ZnO powders with different Co^{2+} doping concentrations (0, 0.5, 1, 3 and 5 mol%) were prepared by the hydrothermal method and characterized by X-ray diffraction (XRD), scanning electron microscopy (SEM), UV–vis diffuse reflectance spectrometer, and photochemical reaction instrument. The results show that the ZnO powders are hexagonal wurtzite structures and their crystallization decrease with the increase of Co^{2+} doping concentration. The products are spherical which have diameter of about 200 nm, and their absorption edge shift to longer wavelength with the increase of the Co^{2+} concentration. The photocatalytic activities of the powders are evaluated using a basic organic dye, methyl orange (MO). Compared with undoped ZnO, it is found that the photocatalytic properties of the Co-doped ZnO have been improved greatly. When the doping concentration is 3 mol%, the degradation ratio of MO can reach 78% after reacting for 240 min.

1. Introduction

Recently, metal-oxide photocatalysts have become a focus of attention due to their possible application to degradation of environmental organic pollutants and the conversion of solar-energy [1,2]. As a suitable alternative photocatalyst to TiO_2, ZnO has a similar band gap energy (3.2 eV) to TiO_2 [3], larger quantum efficiency and higher photocatalytic efficiencies than TiO_2 [4,5]. It has also suggested that ZnO costs lower than TiO_2 for decolorization of organics in aqueous solutions [6]. However, the photocatalytic decolorization can only proceeds under UV irradiation because its wide band gap and absorb UV light with $\lambda < 387$ nm [7]. Unfortunately solar spectrum consists only 5–7% of UV light, the other 46% and 47% of the spectrum are visible light and infrared radiation, respectively [8]. This minimal extent of UV light in the solar spectrum has particularly ruled out the use of natural source of light for photocatalytic decomposition of inorganic contaminants and bacteria disinfection from water and air on large scale [9].

Therefore, in order to shift the optical absorption of ZnO into the visible region and prevent charges from the recombination on the photocatalysts surface, various attempts have been made. For example, it can be achieved by doping transitional metal ions, such as La, Ni, Mn and Fe, or by doping N and S [10–13]. ZnO doped with Mn has been reported to cause hyperchromic shift in the optical absorption of ZnO, which is attributable to the shrinkage of the band gap. This change in ZnO caused by Mn^{2+} was assumed to play an important role in the photocatalysis [9]. In addition, enhancement in the optical absorption owing to the increase of defects in surface layer by doping with Pb^{2+} and Ag^{+} urges us to further investigate both undoped and doped ZnO nanoparticles and their photocatalytic activities [14,15]. Here, ZnO powders doped with Co^{2+} were prepared, and the photocatalytic activities were studied using visible light as radiation source radiation and *methyl orange* as test contaminant.

2. Experimental

2.1. Chemicals

Zinc nitrate hexahydrate ($Zn(NO_3)_2{\cdot}6H_2O$) (analytical grade, Shanghai Chemical Reagent Ltd.), cobalt nitrate hexahydrate ($Co(NO_3)_2{\cdot}6H_2O$) (analytical grade, Shanghai Chemical Reagent Ltd.) were used as zinc and cobalt sources, respectively. Sodium hydroxide (NaOH) was purchased from Tianjin Bodi Ltd. (analytical grade). Methyl orange (MO $C_{14}H_{14}N_3NaO_3S$) (Shanghai Chemical Reagent Factory) was used as indicator. All solutions were prepared with distilled water.

2.2. Preparation of photocatalysts

ZnO powders with different Co^{2+} doping concentrations (0, 0.5, 1, 3 and 5 mol%) were prepared by the hydrothermal method. Usually, $Zn(NO_3)_2{\cdot}6H_2O$ and $Co(NO_3)_2{\cdot}6H_2O$ were dissolved in distilled water to obtain 0.2 mol/L mix solutions (Co^{2+} is x mol%, $x = 0, 0.5, 1, 3$ and 5). 20 mL of 2 mol/L sodium hydroxide solution was slowly added into above-mentioned mix solutions, stirred at room temperature for 30 min, and then moved to a Teflon-lined stainless steel autoclave of 90 mL capacity. The sealed tank was put into an oven and heated at 60 °C for 12 h. When the reactions were completed, the autoclave was cooled to room temperature naturally. Products were collected by filtration, washed with deionized water and alcohol several times, and finally dried in air at 60 °C for 5 h.

* Corresponding author. Tel.: +86 532 66781901; fax: +86 532 66781320.
E-mail address: caolixin@mail.ouc.edu.cn (L. Cao).

0925-8388/$ – see front matter © 2010 Elsevier B.V. All rights reserved.
doi:10.1016/j.jallcom.2010.03.076

2.3. Characterization

The powder X-ray diffraction (XRD) patterns of the samples were recorded by a BRUKER D8 ADVANCE X-ray diffractometer using Cu Kα radiation. Microstructures and morphologies were investigated by a JSM-6700F scanning electron microscopy (SEM). Diffuse reflection spectra were obtained using an UV–vis spectrometer (UV-2450).

2.4. Photocatalytic reactor and degradation procedure

Photochemical reactor was made up of a halogen tungsten lamp (200 W, $400 < \lambda < 700$ nm), a magnetic stirrer and a beaker. 200 mg Co-doped ZnO powders were added into 200 mL MO aqueous solution (10 mg/L) and dispersed under ultrasonic vibration for 10 min. The obtained suspension was continuously stirred for about 0.5 h in darkness to ensure the establishment of an adsorption-desorption equilibrium between the photocatalysts and the MO aqueous solution. Then visible light irradiation started. At regular irradiation intervals, about 5 mL of the mixture was withdrawn, and the catalysts were separated from the suspensions by centrifugation. The degradation process was monitored by an UV–vis absorption spectrometer (measuring the absorption of MO at 463 nm).

3. Results and discussion

3.1. XRD patterns of ZnO and Co-doped ZnO

XRD patterns of ZnO and Co-doped ZnO with different cobalt contents are shown in Fig. 1. All of the diffraction peaks match the

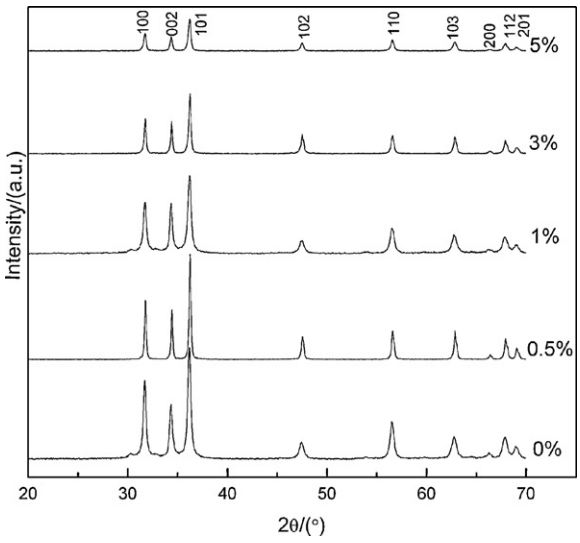

Fig. 1. XRD patterns of doped ZnO prepared with different concentration of Co^{2+}.

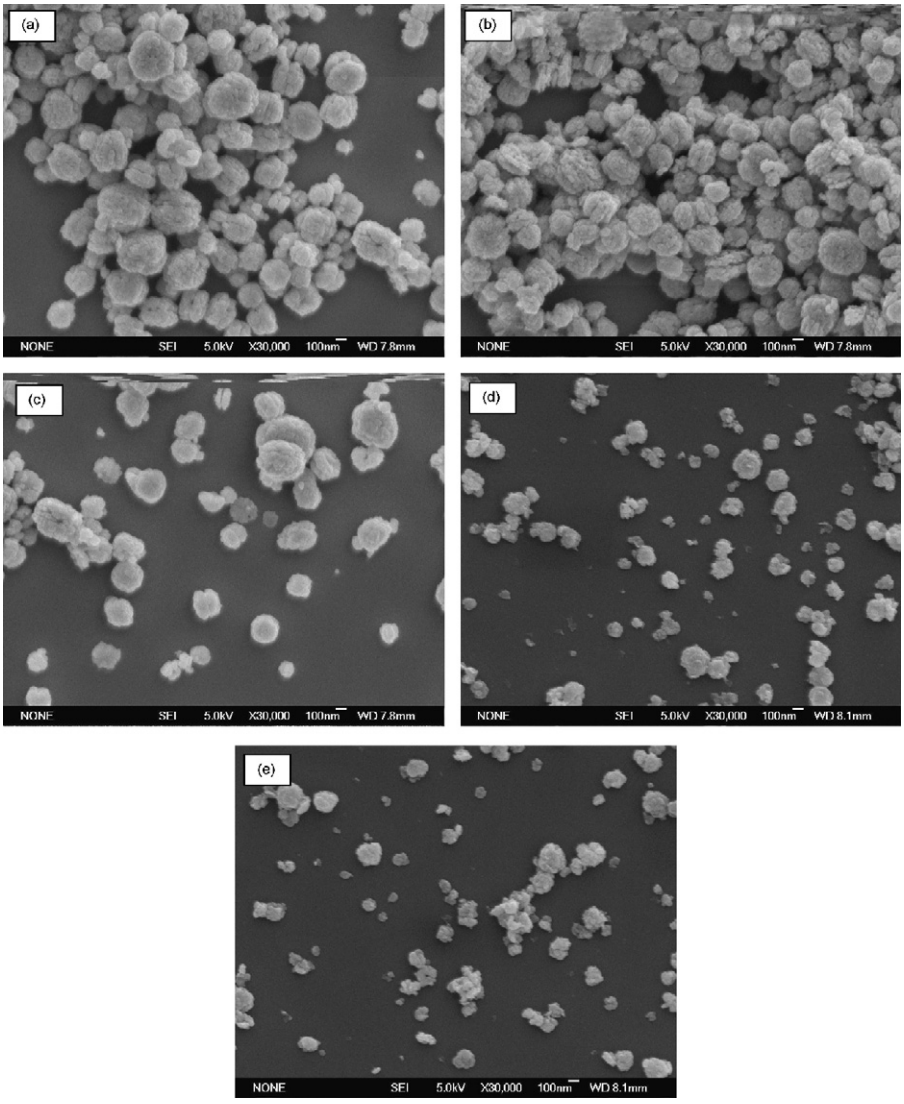

Fig. 2. SEM images of undoped and Co-doped ZnO prepared with different Co^{2+} doping concentrations: (a) 0%, (b) 0.5%, (c) 1%, (d) 3%, and (e) 5%.

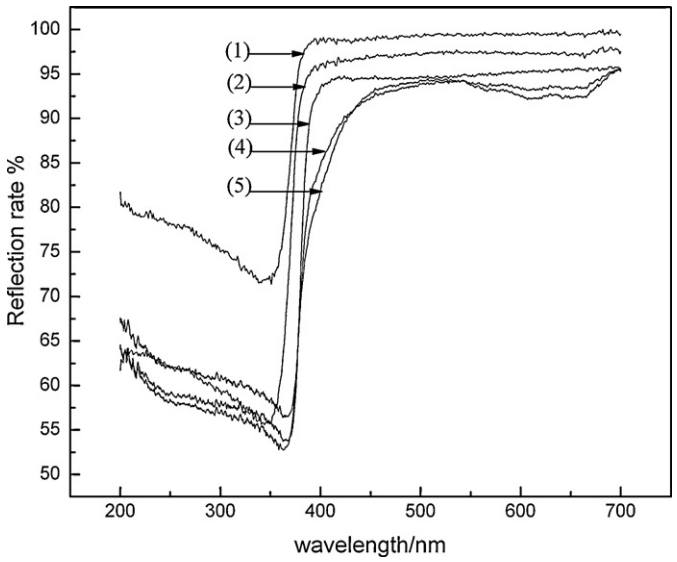

Fig. 3. UV–vis diffuse reflection spectra of undoped and Co-doped ZnO prepared with different Co^{2+} doping concentrations: (a) 0%, (b) 0.5%, (c) 1%, (d) 3%, and (e) 5%.

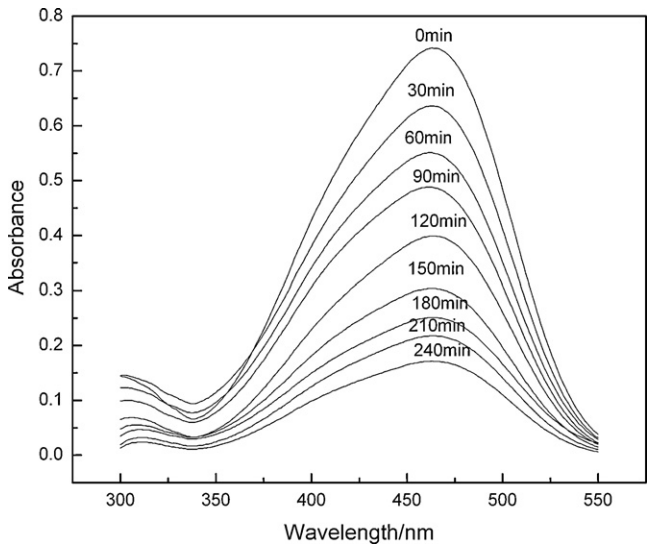

Fig. 4. UV–vis absorption spectra of MO after different irradiation times using Co-doped ZnO powders as photocatalysts.

standard data for a hexagonal ZnO wurtzite structure (JCPDS 36-1451), which demonstrates that doped Co^{2+} ions have no effects on the crystal structure. However, the intensity of the diffraction peaks becomes weaker and the half peak width becomes wider with the increase of the Co^{2+} doping concentration, which implies that the Co^{2+} ions inhibit the aggregating growth of the ZnO particles and influent the crystallization of the ZnO. In addition, it is found that no characteristic peaks of Co or cobalt oxide are detected in all the patterns, which maybe demonstrate that Co^{2+} ions either have entered into the lattices of ZnO substituting of Zn^{2+} or existed in the form of amorphous [16].

3.2. SEM images of ZnO and Co-doped ZnO

To obtain detailed information about the microstructure and morphology of the synthesized samples, Scanning electron microscopy (SEM) was carried out. The result is shown in Fig. 2. As shown in the pictures, the morphology of the products have not any change with the increase of the Co^{2+} doping concentration. All the products which the diameter ranges from 100 to 300 nm are spherical and their surface is very rough. In addition, it is found that, the size of the products become smaller with the increase of the Co^{2+} doping concentration.

3.3. UV–vis diffuse reflectance analysis

The UV–vis diffuse reflectance spectra of undoped ZnO and Co-doped ZnO are shown in Fig. 3. It is found that the reflection rate of the undoped ZnO begins to decrease at 380 nm, while the band edge of the Co-doped ZnO sample shifted to longer wavelengths with the increase of the Co^{2+} doping concentration. The red shift of the band edge with the incorporation of Co into ZnO has been observed [17] and ascribed to the sp–d exchange interactions between the band electrons and the localized d electrons of the Co^{2+} ions which substitute Zn^{2+} ions [18]. The s–d and p–d exchange interactions led to a negative and a positive correction to the conduction band and the valence band edges separately, resulting in a band gap narrowing [19]. In addition, the reflection rate of the Co-doped ZnO in visible light range decreases with the increase of the Co^{2+} doping concentration. When the doping concentration reaches 3%, the reflection rate in visible light range decreases to 90% and a strong absorption between 600 and 700 nm can be observed, which has very important signification in making full use of sunlight.

3.4. Photocatalytic degradation of MO

MO was used as a test contaminant, because its absorption peak is in the visible range and its degradation can be easily monitored by optical absorption spectroscopy. Fig. 4 shows the UV–vis absorption spectra of MO at different irradiating intervals using the Co-doped ZnO powders as photocatalysts, the Co^{2+} concentration is 3%. From the figure, it is found that the absorption peak of the MO is at 463 nm and the intensities decrease with the increase of the irradiation time, the absorbance intensity reduced to 0.171 after 240 min irradiation. It indicates that the concentration of MO in the solution is reduced gradually.

Curves of methyl orange degradated by ZnO powders with different Co^{2+} doping concentrations are shown in Fig. 5. It is found that undoped ZnO has a little ability to mineralize MO under the

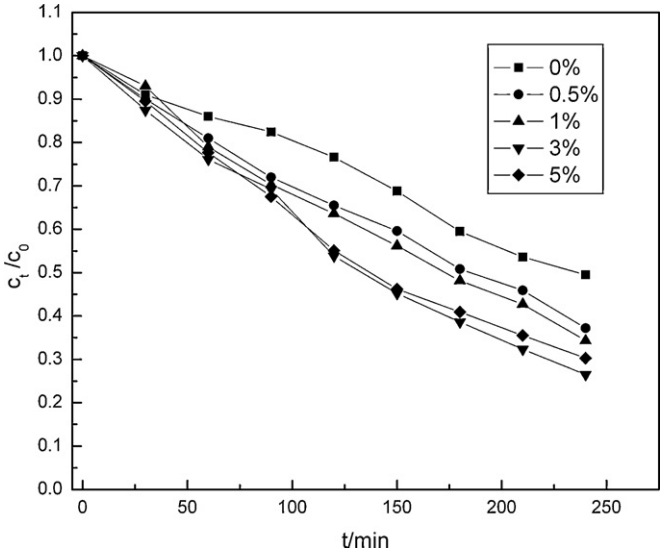

Fig. 5. Degradation curves of MO using Co-doped ZnO powders with different Co^{2+} concentrations as photocatalysts. (C_0 is the initial concentration of MO, C_t is the concentration of MO after 't' minutes.).

visible light irradiation. However, all of the Co-doped ZnO photocatalysts exhibits higher photocatalytic activity than the undoped ZnO. This may be attributed both to the better performance of the absorption in visible light range and to the larger the content of oxygen vacancies or defects which produced by doping Co^{2+} [19]. During the 240 min irradiation, the order of the photocatalytic activities of the Co-doped ZnO with different Co^{2+} doping concentrations is as followings: 3 > 5 > 1 > 0.5 > 0 mol%. The 3 mol% Co-doped ZnO photocatalyst exhibits the highest photocatalytic decolorization efficiency, MO concentration reduced as much as 78% after 240 min, which suggests that the doping of Co^{2+} may enhance the photocatalytic activity of ZnO and there is an optimum doping concentration of Co^{2+} ions in ZnO.

4. Conclusions

Co-doped ZnO photocatalysts were prepared by hydrothermal method. The powders are spherical in shape belonging to hexagonal wurtzite structures. The absorption edge shifted to longer wavelengths with the increase of the cobalt concentration. Co-doped ZnO photocatalyst owned improved photocatalytic activity in decolorization of MO under visible light irradiation. The 3 mol% Co-doped ZnO photocatalyst exhibits the highest photocatalytic decolorization efficiency, leading to as much as 78% reduction of the MO concentration in 240 min. All these indicated that Co-doped ZnO was a potential candidate for the practical application in photocatalytic decolorization of organic contaminants.

Acknowledgement

We thank the National Science Foundation of China (NSFC 50672089) and Program for New Century Excellent Talents in University (NCET-08-0511) for financial support.

References

[1] X.X. Fan, X.Y. Chen, S.P. Zhub, J. Mol. Catal. A: Chem. 284 (2008) 155–160.
[2] D.A. Tryk, A. Fujishima, K. Honda, Electrochim. Acta 45 (2000) 2363–2376.
[3] S. Sakthivel, B. Neppolian, M.V. Shankar, B. Arabindoo, M. Palanichamy, V. Murugesan, Sol. Energy Mater. Sol. Cells 77 (2003) 65–82.
[4] K. Gouvea, F. Wypych, S.G. Moraes, N. Duran, N. Nagata, P. Peralta-Zamora, Chemosphere 40 (2000) 433–440.
[5] S. Chakrabarti, B. Chaudhuri, S. Bhattacharjee, J. Hazard. Mater. 154 (2008) 230–236.
[6] N. Daneshvar, D. Salari, A.R. Khataee, J. Photochem. Photobiol. A 162 (2004) 317–322.
[7] N. Serpone, D. Lawless, J. Disdier, J.M. Herrmann, Langmuir 10 (1994) 643–652.
[8] T Bak, J. Nowotny, M. Rekas, C.C. Sorrell, Int. J. Hydrogen Energy 27 (2002) 1022–2799.
[9] R. Ullah, Joydeep, J. Hazard. Mater. 35 (2008) 4305–4314.
[10] J.T. Chena, J. Wang, J. Cryst. Growth 310 (2008) 2627–2632.
[11] S. Ekambaram, Y. Iikubo, J. Alloys Compd 433 (2007) 237–240.
[12] D. Li, H. Haneda, Thin Solid Films 486 (2005) 20–23.
[13] J.F. Lu, Q.W. Zhang, Powder Technol. 162 (2006) 33–37.
[14] K. Vanhesuden, W.L. Warren, J.A. Voigt, C.H. Seager, D.R. Tallant, Appl. Phys. Lett. 67 (1995) 1280–1282.
[15] R. Wang, J.H. Xin, Y. Yang, H. Liu, L. Xu, J. Hu, Appl. Surf. Sci. 227 (2004) 312–317.
[16] M. Bouloudenine, N. Viart, S. Colis, A. Dinia, Chem. Phys. Lett. 397 (2004) 73–76.
[17] C.B. Fitzgerald, M. Venkatesan, J.G. Lunney, L.S. Dornelse, J.M.D. Coey, Appl. Surf. Sci. 247 (2005) 493–496.
[18] Y.D. Kim, S.L. Cooper, M.V. Klein, B.T. Jonker, Phys. Rev. B 49 (1994) 1732–1742.
[19] Q. Xiao, J. Zhang, Mater. Sci. Eng. B 142 (2007) 121–125.